ADV MATH SCI JOURNAL
Advances in Mathematics: Scientific Journal 8 (2019), no.3, 109–130
(Special issue on ICRAPAM)
ISSN 1857-8365 printed version
ISSN 1857-8438 electronic version

A MATHEMATICAL STUDY ON MHD BOUNDARY LAYER FLOW OF NANOFLUID AND HEAT TRANSFER OVER A POROUS EXPONENTIALLY STRETCHING SHEET

V. Ananthaswamy[1], C.Sumathi[2], V.K.Shanthi[3]

[1]PG & Research Department of Mathematics, The Madura College,

Madurai,Tamilnadu,India.

[2]Research Scholar, Sri Meenakshi Govt Arts College for Women, Madurai,Tamilnadu,India

[3]Department of Mathematics, Sri Meenakshi Govt Arts College for Women,

Madurai,Tamilnadu,India.

Corresponding author e-mail: ananthu9777@rediffmail.com

Abstract :A mathematical analysis of the steady boundary layer flow of nanofluid due to anexponentially stretching sheet with magnetic field in presence of chemical reaction, thermal radiation and viscous dissipation is presented.The approximate analytical expressions ofthe dimensionless velocity, dimensionless temperature and dimensionless concentration profiles are derived analytically and graphically by using the New Homotopy analysis method. The effect of various prominent parameters local like skin friction, local Nusselt number and local Sherwoodnumber are also derived analytically and graphically. Numerical values of different involved parameters on the local skin friction coefficient, local Nusselt and Sherwood numbers are obtained and compared with our analytical results.A satisfactory agreement between analytical and numerical results are noted.

Keywords: Chemical reaction; MHD; Heat and mass transfer; Micropolar; Modified Homotopy analysis method.

1. Introduction

The magnetohytrodynamic (MHD) flow is the influence of a magnetic field on the viscous flow of electrically conducting fluid. This fluid plays a vital role in many manufacturing processes, such as in MHD electrical power generation, magnetic materials processing, glass manufacturing, and purification of crude oil, paper production and geophysics. The cooling rate can be controlled by using MHD. The desired quality of the product can be achieved by MHD. Owing to its various applications in the manufacturing processes, the study of magnetohytrodynamic (MHD) boundary layer flow on a constant stretching sheet is given attention for the last few decades. The former to learn the boundary

layer flow caused by a stretching sheet which moves with a velocity varying linearly with the distance from a fixed point was Crane [2].With external magnetic field, viscous dissipation and Joule Effects, the MHD flow and heat transfer over stretching/shrinking sheets is studied by Jafar et al. [3].Over a stretching sheet, Prasad et. al. [4] explained the effect of variable viscosity on MHD viscous-elastic fluid flow and heat transfer. On a linearly stretching sheet, Sharma et.al. [5] discussed the effects of variable thermal conductivity and heat source/sink on MHD flow near a stagnation point. While probing the coolants techniques and cooling processes, Choi coined the term Nanofluid at Argonne National Laboratory in US. The nanometer sized particles of oxides, metals, carbides or carbon nanotubes are defined as Nanofluid. As convective properties and thermal conductivity of the Nanofluid is dominant over the properties of the base fluid, the properties of Nanofluid are significant over base fluid. Water, toluene, ethylene glycol, and oil are common base fluids. Over the base fluid, thermal conductivity is more efficiently better in the range of 15% - 40%. Many researchers worldwide are involved in the study of nanofluid. For example, in transportation, nuclear reactor, electronics as well as biomedicine and food, this nanofluid is used. With nanoparticles, the Enhancing thermal conductivity of fluids is analyzed byChoi [6] andKhan et.al [7] studied the boundary layer flow of nanofluids over a stretching surface. With suction/injection, the effect of MHD flow over a permeable stretching/shrinking sheet of a nanofluid is discussed by SandeepNaramgariet.al [8].SohailNadem et.al [9] studied the boundary layer flow of nanofluid over an exponentially stretching surface.In a nanofluid, NorfifahBachok et.al, [10] explained the boundary layer stagnation-point flow and heat transfer over an exponentially stretching/shrinking sheet. With velocity, thermal and solute slip boundary conditions, the MHD boundary layer flow and heat transfer of a nanofluid over a permeable stretching sheet is presented by Wubshet Ibrahim et.al, [11] and Rashid et. al, [12] examined the Homotopy simulation of nanofluid dynamics from a non-linearly stretching isothermal permeable sheet with transpiration.The method of converting mechanical energy of downward-flowing water into acoustical and thermal energy is called dissipation. In order to lessen the kinetic energy of flowing waters and reducing their erosive potential on streambeds, many devices are developed in the banks and river bottoms. Viscous dissipation is used in many applications in polymer processing flows such as extrusion at high rates or injection modeling, considerable temperature rises are seen. Mohsen Sheikholeslami et. al [13] explained the numerical simulation of MHD nanofluid flow and heat transfer by considering viscous dissipation. With viscous dissipation, Sin Wei Wong et al. [14] studied the Boundary layer flow and heat transfer over an exponentially stretching/shrinking permeable sheet. Using chemical reaction effects and viscous dissipation, Heat and mass transfer in MHD flow of nanofluids through an absorbent media due to a permeable stretching sheet is analyzed by YohannesYirgaet.al, [15].In the blueprint of many higher energy conversion systems operating at high temperature, the effect of thermal radiation on flow and heat transfer processes play an important role.Within the energy conversion system, the thermal radiations arise due to the emission by the working fluid and hot walls. Boundary layer flow over a stretching surface in association with transverse magnetic field and thermal radiation within nanofluid medium flow is vital due to its application in various industries, for instance in the design of dependable equipment's, polymer and processing engineering, petrochemical industry ,metallurgy , gas turbines, nuclear plants and many propulsion devices for aircraft, satellites, space vehicles and missiles.Over a permeable plate, the heat transfer analysis of MHD nanofluid flow is discussed by Mutuku-Njane et.al [16].Fekry M Hady et al. [17] presented heat transfer over a nonlinearly stretching sheet and radiation effect on viscous flow of a nanofluid in porous medium, over a stretching sheet, Liancun Zhenga et al. [18] studied radiation heat transfer of a nanofluid with velocity slip and temperature jump.Thermal radiation effect on the nanofluid buoyancy flow and heat transfer over a stretching sheet is analyzed by Abdul Sattar Dogonchi et.al [19].Radiation and MHD boundary layer stagnation-point of nanofluid flow towards a stretching sheet rooted in a porous medium is investigated by Emad H. Aly [20].With dissipation effect, Maria Imtiaz et. al,[21] explained the flow of magneto nanofluid by a radiative exponentially stretching surface.In a porous medium with heat generation and viscous dissipation, the effect of mixed convection–radiation on stagnation-point flow of nanofluids over a stretching/shrinking sheet is presented by Dulal Pal et.al [22]. In the presence of nanofluids, the study of heat transfer with chemical reaction gained a great value in the many branches of science and engineering. This is commonly seen in heat exchanger design Petro-chemical industry, cooling of nuclear reactors, cooling systems and power, chemical vapor, deposition on surfaces, geophysics and forest fire dynamics as

well as in magneto hydrodynamic power generation system.Over an exponentially stretching sheet, the influence of chemical reaction and thermal radiation on MHD boundary layer flow and heat transfer of a nanofluid is discussed by Rudraswamy et.al [23].Mohamed R.Eid [24] presented the influence of chemical reaction on MHD boundary-layer flow of two-phase nanofluid model with a heat generation over an exponentially stretching sheet.Das et al. [25] explained the mixed convection and nonlinear radiation in the stagnation point nanofluid flow towards a stretching sheet with homogenous-heterogeneous Reactions effects. With thermal radiation and chemical reaction, the Heat and mass transfer analysis of nanofluid over linear and non-linear stretching surfaces is studied bySreedevi et.al, [26].

2. Mathematical formulation of the problem

We consider a steady two-dimensional flow an incompressible viscous and electrically conducted nanofluid caused by a stretching sheet,which is placed in a quiescent ambient fluid of uniform temperature of the plate and species concentration to $T_w > T_\infty$ and $C_w > C_\infty$ are temperature and Species concentration at the wall and C_∞, T_∞ are the temperature and species concentration for away from the platerespectively .The *x*-axis is taken along the stretching sheet in the direction of the motion and y-axis is perpendicular to it. Consider that a variable magnetic field $B(x)$ is applied normal to the sheet that the induced magnetic field is neglected, which is justified for MHD flow at small magnetic Reynolds number. A physical model of the
problem shown in Fig.1.

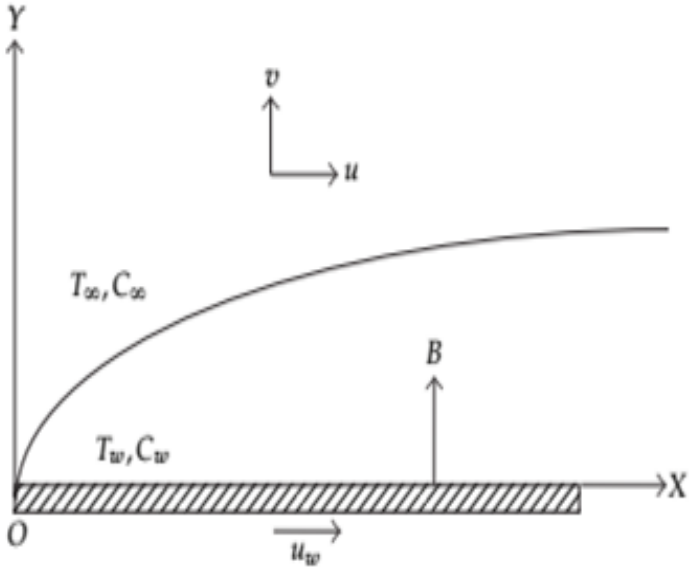

Fig. 1: Physical model and coordinate system

Under the above assumptions and useful boundary layer approximation, the steady MHD boundary layer flow of nanofluid flow an exponentially stretching sheet in presence of chemical reaction and thermal radiation are governed by the flowing equation of momentum, energy and species concentration are written in common notation as:

$$\frac{\partial u}{\partial x} + \frac{\partial u}{\partial x} \tag{1}$$

$$u\frac{\partial u}{\partial x} + v\frac{\partial u}{\partial y} = u\frac{\partial^2 u}{\partial y^2} - \frac{\sigma B^2}{\rho_f}u - u\frac{v}{K} \tag{2}$$

$$u\frac{\partial T}{\partial x} + v\frac{\partial T}{\partial y} = \alpha\frac{\partial^2 T}{\partial y^2} - \frac{\sigma B^2}{\rho_f}u - \frac{v}{c_P}\left(\frac{\partial u}{\partial y}\right)^2 + \tau\left\{D_B\frac{\partial T}{\partial y}\frac{\partial C}{\partial y} + \frac{D_T}{T_\infty}\left(\frac{\partial T}{\partial y}\right)^2\right\} - \frac{1}{(\rho C)_f}\frac{\partial q_r}{\partial y} \tag{3}$$

$$u\frac{\partial C}{\partial x}+v\frac{\partial C}{\partial y}=D_B\frac{\partial^2 C}{\partial y^2}+\frac{D_T}{T_\infty}\frac{\partial^2 T}{\partial y^2}-K_0(C-C_\infty) \quad (4)$$

where u and v are the velocity components in x - and y -directions, respectively, v is the kinematic viscosity, ρ_f is the density of the base fluid, T is the temperature, T_∞ is constant temperature of the fluid in the in viscid free stream, α is the thermal conductivity, ρC_P is the effective heat capacity of nanoparticles, ρC_f is heat capacity of the base fluid, C is nanoparticles volume fraction, K is the permeability of the porous medium, D_B is the Brownian diffusion coefficient, D_T is the thermophoretic diffusion coefficient, C_P is the specific heat at constant pressure. Here, the variable magnetic field $\mathrm{B}(\mathrm{x})$ is taken in the form

$$B(x)=B_o\, e^{\left(\frac{x}{2L}\right)} \quad (5)$$

We are assumed that the permeability K of the porous medium of the following form

$$K(x)=2k_o\, e^{\left(\frac{-x}{L}\right)} \quad (6)$$

The boundary conditions are as follows

$$\begin{aligned} &u=U_w(x), v=v_w, T=T_w=T_\infty+T_0 e^{\left(\frac{x}{2l}\right)} \\ &C=C_w=C_\infty+C_0 e^{\frac{x}{2l}} \qquad at\ y=0 \\ &u\to 0, T\to T_\infty, C\to C_\infty \qquad at\ y\to\infty \end{aligned} \quad (7)$$

where T_w is the variable temperature at the sheet with T_0 being a constant which measure the rate of temperature increase along the sheet, C_w the variable wall nano-particle volume fraction with C_0 being a constant C_∞ is constant nano-particle volume fraction in free stream. The stretching U_w velocity is given

$$U_w(x)=c\, e^{\left(\frac{x}{L}\right)} \quad (8)$$

where $C>0$ is stretching sheet.

Now V_w is a variable wall mass transfer velocity and it is given by the form

$$V_w(x)=V_0\, e^{\left(\frac{x}{2L}\right)} \quad (9)$$

where V_0 is called constant and $V_0>0$ for mass suction $V_0<0$ for mass injection the radiative heat flux in the x-axis is considered negligible as compared to y-axis. Hence, by using Roseland approximation for radiation, the radiative heat flux q_r is given by

$$q_r=-\frac{4\sigma^*}{3k^*}\frac{\partial T^4}{\partial y} \quad (10)$$

where k^* is the mean absorption coefficient, σ^* is called Stefan-Boltzmann,now consider the temperature difference with in the flow sufficiently small term T^4 may be extend to the linear function of temperature. This is completed by expending T^4 Taylor's series about a free stream temperature T^∞ and ignore the higher order terms we get

$$T^4\approx 4T_\infty^3 T-3T_\infty^4 \quad (11)$$

$$q_r = -\frac{16\sigma^* T_\infty^3}{3k^*}\frac{\partial T}{\partial y}$$
$$\frac{\partial q_r}{\partial y} = -\frac{16\sigma^* T_\infty^3}{3k^*}\frac{\partial^2 T}{\partial y^2} \qquad (12)$$

Now we introduce the similarity transformations as follows:

$$\psi = \sqrt{2\nu L\ c}\, f(\eta) e^{\left(\frac{x}{2L}\right)}, \theta(\eta) = \frac{T - T_\infty}{T_w - T_\infty}, \phi(\eta) = \frac{C - C_\infty}{C_w - C_\infty}, \eta = y\sqrt{\frac{c}{2\nu L}}\, e^{\left(\frac{x}{2L}\right)} \qquad (13)$$

ψ is astream function with $u = \frac{\partial \psi}{\partial y}, v = \frac{\partial \psi}{\partial x}$ and η is called similarity variable using the eqn. (15), theeqns. (1)-(3) are transformed to the following ordinary differential eqns.

$$f''' - 2f' + Sf'' - (M + K1) f' = 0 \qquad (14)$$

$$\theta'' + \frac{\Pr}{\left(1 + \frac{4}{3}R\right)}\left[\left(S\theta' - \theta + Ec\left(f''\right)^2 + Nb\,\theta'\phi' + Nt\left(\theta'\right)^2\right)\right] = 0 \qquad (15)$$

$$\phi'' + Le\left(S\phi' - \phi\right) + \frac{Nt}{Nb}\theta'' - Le\,\gamma\,\mathrm{Re}_x\,\phi = 0 \qquad (16)$$

where $M = \frac{2\sigma {B_0}^2}{c\rho}$ is called Magnetic parameter, $\Pr = \frac{\nu}{\alpha}$ is a Prandtl Number, $Ec = \frac{c^2 e^{\left(\frac{x}{2L}\right)}}{(T_w - T_\infty)(C_P)_f}$ is called the Eckert number, $K1 = \frac{CK0}{\nu L}$ is the permeability parameter, $R = \frac{4\sigma^* T_\infty^3}{kK^*}$ is called radiation parameter, $\gamma = \frac{\nu K_0}{U_w^2}$ is the chemical reaction parameter, $\mathrm{Re}_x = \frac{xU_w}{\nu}$ is called local Reynolds number .The dimensionless parameters Nb (Brownian motion parameter)and Nt (Thermophoresis parameter) are defined as follows:

$$Nb = D_B \frac{(\rho c)_P}{(\rho c) f}\frac{C_w - C_\infty}{\nu}, Nt = \frac{D_T}{T_\infty}\frac{(\rho c)_P}{(\rho c) f}\frac{T_w - T_\infty}{\nu} \qquad (17)$$

The boundary conditions (7) reduce to following form:

$$\begin{aligned} &f(\eta) = S, f'(\eta) = 1, \theta(\eta) = 1, \phi(\eta) = 1 && at\ \eta \to 0 \\ &f'(\eta) = 0, \theta(\eta) = 0, \phi(\eta) = 0 && at\ \eta \to \infty \end{aligned} \qquad (18)$$

where

$S = {-v_0}\Big/\sqrt{\frac{\nu c}{2L}}$ iscalled wall mass transfer parameter, $S > 0(v_0 < 0)$ corresponds to mass suction and $S < 0(v_0 > 0)$ corresponds to mass injection. The quantities of physical interest for this problem are the local skin friction C_f, the local Nussel tnumber Nu_x and the local sherwood number Sh_x.These all are defined as follows:

$$C_f = \frac{\nu}{U_w e^{\left(\frac{x}{2L}\right)}}\frac{\partial u}{\partial y}\Big| y = 0, Nu_x = \frac{x}{(T_w - T_\infty),}\frac{\partial T}{\partial y}\Big| y = 0, Sh_x = \frac{x}{(C_w - C_\infty),}\frac{\partial C}{\partial y}\Big| y = 0 \qquad (19)$$

That is

$$f''(0)=\sqrt{2\,\mathrm{Re}_x\,C_f}\,,\ \frac{Nu_x}{\sqrt{2\,\mathrm{Re}_x}}=-\sqrt{\frac{x}{2L}}\theta'(0),\ \frac{Sh_x}{\sqrt{2\,\mathrm{Re}_x}}=-\sqrt{\frac{x}{2L}}\phi'(0) \qquad (20)$$

3. Solution of the non-linear differential equations using the Modified Homotopy analysis method

Homotopy analysis method (HAM) is a non -perturbative analytical method for obtaining series solutions to nonlinear equations and has been successfully applied to numerous problems in science and engineering. In comparison with other perturbative and non -perturbative analytical methods, HAM offers the ability to adjust and control the convergence of a solution via the so-called convergence-control parameter. Because of this, HAM has proved to be the most effective method for obtaining analytical solutions to highly non-linear differential equations. Previous applications of HAM have mainly focused on non-linear differential equations in which the non-linearity is a polynomial in terms of the unknown function and its derivatives. As seen in (1), the non-linearity present in electrohydrodynamic flow takes the form of a rational function, and thus, poses a greater challenge with respect to finding approximate solutions analytically. Our results show that even in this case, HAM yields excellent results.

Liao [25-33] proposed a powerful analytical method for non-linear problems, namely the Homotopy analysis method. This method provides an analytical solution in terms of an infinite power series. However, there is a practical need to evaluate this solution and to obtain numerical values from the infinite power series. In order to investigate the accuracy of the Homotopy analysis method (HAM) solution with a finite number of terms, the system of differential equations was solved. The Homotopy analysis method is a good technique comparing to another perturbation method. The Homotopy analysis method contains the auxiliary parameter h, which provides us with a simple way to adjust and control the convergence region of solution series. The approximate analytic solution of the eqns. (14)-(16) by using the Modified Homotopy analysis method (MHAM) is as follows:

$$f(\eta)=e_1+e_2\,e^{G\eta}+e_3\,e^{-G_1\eta} \qquad (21)$$

$$f'(\eta)=Ge_2\,e^{G\eta}-G_1e_3\,e^{-G_1\eta} \qquad (22)$$

$$\theta(\eta)=r_1\,e^{L\eta}+r_2\,e^{-L\eta}-h\left(\begin{array}{l}\left(r_3\,e^{L\eta}+r_4\,e^{-L\eta}\right)\\ +\dfrac{\mathrm{Pr}}{\left(1+\dfrac{4}{3}R\right)}\left[\begin{array}{l}s\left(\dfrac{-L\,e^{-L\eta}}{L^2-L}\right)+\dfrac{c^2\,Ec\,e^{-2c\eta}}{\left(4c^2-L\right)}\\ +Nb\left(\left(\dfrac{-L\,e^{-L\eta}}{L^2-L}\right)\left(\dfrac{-B\,e^{-B\eta}}{B^2-L}\right)\right)\\ Nt\left(\dfrac{L^2e^{-2L\eta}}{\left(4L^2-L\right)}\right)\end{array}\right]\end{array}\right) \qquad (23)$$

$$\phi(\eta)=c_1\,e^{B\eta}+c_2\,e^{-B\eta}-h\left[c_3\,e^{B\eta}+c_4\,e^{-B\eta}-\frac{Le\,S\,B\,e^{-B\eta}}{B^2-B}-\frac{Nt}{Nb}\frac{L^2e^{-L\eta}}{L^2-B}\right]. \qquad (24)$$

The analyticalexpression of the local skin friction given by

$$f''(0)=-(-G_1). \qquad (25)$$

The analytical expression of the local nusselt number is as follows:

$$\theta'(0) = -\left(r_1 L - r_2 L - h\left(a_3 L - a_4 L + \frac{\Pr}{\left(1+\frac{4}{3}R\right)}\left(\begin{array}{l} \frac{S L^2}{\left(L^2 - L\right)} \\ -2\frac{c^3 Ec}{\left(4c^2 - L\right)} - \frac{NbL^2 B}{\left(B^2 - L\right)\left(L^2 - L\right)} \\ -\frac{NbLB^2}{\left(B^2 - L\right)\left(L^2 - L\right)} - 2\frac{L^3 Nt}{\left(4L^2 - L\right)} \end{array} \right) \right) \right) \quad . \qquad (26)$$

The analytical expression of the local Sherwood number is given by:

$$\phi'(0) = -\left(-B - h\left(c_1 B - c_2 B + \frac{Le\, S\, B^2}{B^2 - B} + \frac{L^3 Nt}{Nb\left(L^2 - B\right)} \right) \right) \qquad (27)$$

where

$$e_1 = S + \frac{1}{G_1}, e_2 = 0, e_3 = -\frac{1}{G_1} \qquad (28)$$

$$r_1 = 0, r_2 = 1, r_3 = 0, r_4 = -\left(\frac{\Pr}{\left(1+\frac{4}{3}R\right)}\left(-\frac{S\, L}{L^2 - L} + \frac{c^2\, Ec}{4c^2 - L} + \frac{Nb\, L\, B}{\left(L^2 - L\right)\left(B^2 - L\right)} + \frac{L^2\, Nt}{4L^2 - L} \right) \right) \qquad (29)$$

$$c_1 = 0, c_2 = 1, c_3 = 0, c_4 = \frac{Le\, S}{B^2 - B} + \frac{Nt}{Nb}\left(\frac{L^2}{4L^2 - B} \right) \qquad (30)$$

$$B = \sqrt{Le + Le\, R\,\mathrm{Re}}, L = \sqrt{\frac{\Pr}{\left(1+\frac{4}{3}R\right)}}, G_1 = \frac{S + \sqrt{S^2 + 4\left(2 + M + K1\right)}}{2}, \quad . \qquad (31)$$

$$G = \frac{S - \sqrt{S^2 + 4\left(2 + M + K1\right)}}{2}$$

4. Result and discussion

In this paper we derived the analytical expression of the dimensionless velocity profile $f'(\eta)$, dimension less temperature profile $\theta(\eta)$and dimensionless concentration profile $\phi(\eta)$ by using Modified Homotopy analysis method. Fig.1 is the physical model of the fluid flow. Fig.2 represents the dimensionless velocity $f'(\eta)$ verses dimensionless similarity variable(η).From Fig.2 (a), it is evident that when the magnetic parameter M increases, the corresponding dimensionless velocity profiles decreases in some fixed values of the other dimensionless parameters. From Fig. 2(b),it is observed that when the suction parameter S increases, the corresponding the dimensionless velocity profiles decreases in some fixed values of the other dimensionless parameters. From Fig.2(c),it is noted that when the permeability parameter $K1$ increases, the corresponding the dimensionless velocity profiles decreases in some fixed values of the other dimensionless parameters. Fig. 2(d) represents thelocal skin friction $-f''(0)$ verses suction parameter S .From Fig 2(d), it is evident that when the magnetic parameter M increases ,the corresponding local skin friction $-f''(0)$ also increases in some fixed value of the other dimension less parameter.

Fig.3 represents the dimensionless temperature $\theta(\eta)$ verses dimension less similarity variable (η). From Fig. 3(a),it depicts that when the magnetic parameter M increases, the corresponding the dimensionless velocity profiles also increases in some fixed values of the other dimensionless parameters. From Fig.3(b), it is observed that when the suction parameter S increases, the corresponding the dimensionless temperature profiles decreases in some fixed values of the other dimensionless parameters. From Fig.3(c), it is noted that when the Prandtl number $\Pr$ increases, the corresponding the dimensionless temperature profiles decreases in some fixed values of the other dimensionless parameters. From Fig.3(d), it is examined that when the thermophoresis parameter Nt increases, the corresponding the dimensionless velocity profiles alsoincreases in some fixed values of the other dimensionless parameters.From Fig.3(e), it is observed that when the Brownian motion parameter Nb increases, the corresponding the dimensionless velocity profiles increases in some fixed values of the other dimensionless parameters. From Fig. 3(f), it is noted that when the Brownian motion parameter Eckert number Ec increases, the corresponding the dimensionless velocity profiles increases in some fixed values of the other dimensionless parameters.From Fig. 3(g),itis thatexamined that when the radiation parameter R increases, the corresponding the dimensionless velocity profiles alsoincreases in some fixed values of the other dimensionless parameters.

From Fig.4, represents the dimensionless concentration profile $\phi(\eta)$ verses the dimensionless similarity variable (η).From Fig.4(a),it is noted that when the chemical reaction parameter γ increases, the corresponding the dimensionless concentration profiles decreases in some fixed values of the other dimensionless parameters.From Fig.4(b),it is evident that when the thermophoresis parameter Nt increases, the corresponding the dimensionless concentration profiles increases in some fixed values of the other dimensionless parameters.From Fig.4(c), it shows that when the Brownian motion parameter Nb increases, the corresponding the dimensionless concentration profiles decreases in some fixed values of the other dimensionless parameters.From Fig. 4(d), it is notedthat when the lewis number Le increases, the corresponding the dimensionless concentration profiles decreases in some fixed values of the other dimensionless parameters. From Fig.4(e),it reveals that when the suction parameter S increases, the corresponding the dimensionless concentration profiles decreases in some fixed values of the other dimensionless parameters.From Fig. 4(f), we noted that when Brownian motion parameter Nb increases the corresponding local Sherwood number $-\phi'(0)$increases in some fixed value of the other dimensionless parameters.

Table.1 shows that the analytical and numerical values of the local skin friction $-f''(0)$. From this table it is observed that when suction parameter S, magnetic parameter M and permeability parameter $K1$increases.Table.2 representsthe analytical and numerical values of thelocalNusselt number $-\theta'(0)$. From this table it is noted that when suction parameter S, magnetic parameter M ,permeability parameter $K1$,brownian motion parameter Nb ,lewis Number Le ,chemical reaction parameter γ and thermophoresis parameter Nt increases. Table.3 representsthe analytical and numerical values of thelocal sherwood number $-\phi'(0)$.From thistable it is observe that when brownian motion parameter Nb ,lewisnumber Le, chemicalreaction parameter γ and thermophoresis parameter Nt increases.

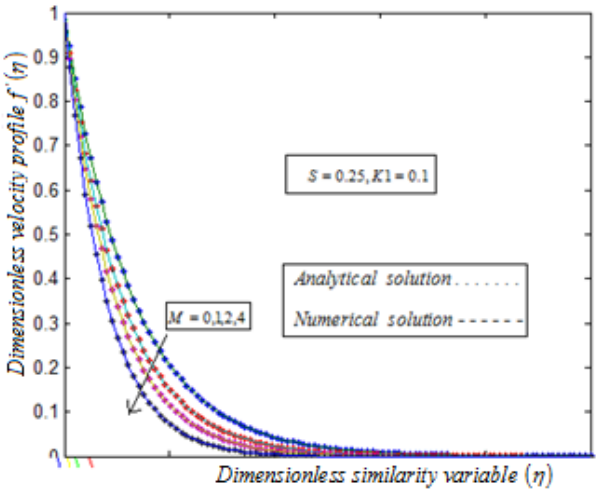

2(a): Dimensionless velocity $f'(\eta)$ verses dimensionless similarity variable (η).The curves are plotted using the eqn. (22) for various valuesof themagnetic parameter M and in some fixed values of the other dimensionless parameters $S, K1$.

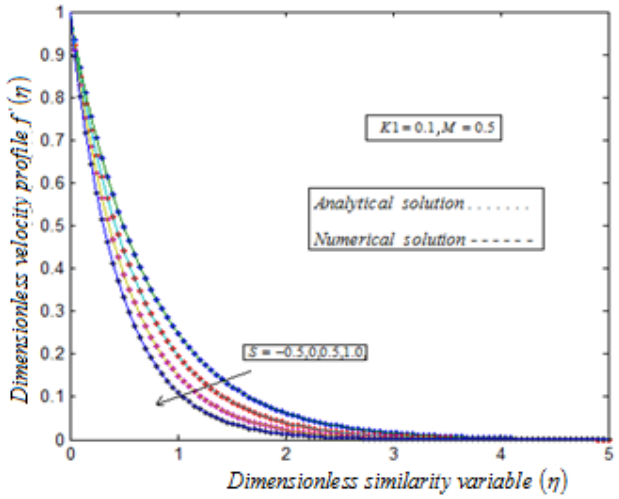

Fig. 2(b): Dimensionless velocity profile $f'(\eta)$ verses the dimensionless similarity variable (η). The curves are plotted using the eqn.(22) for various valuesof the suction parameter S and in some fixed values of the other dimensionless parameter $M, K1$.

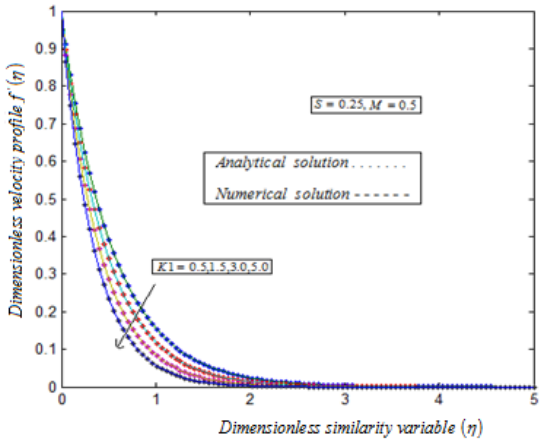

Fig. 2(c): Dimensionless velocity profile $f'(\eta)$ verses the dimensionless similarity variable (η). The curves are plotted using the eqn.(22) for various values of the permeability parameter $K1$ and in some fixed values of the other dimensionless parameters S, M.

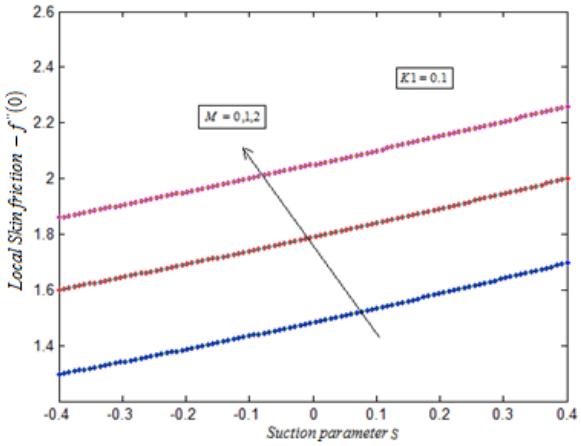

Fig. 2(d): Local skin friction $-f''(0)$ verses suction parameter S .The curves are plotted using the eqn.(25) for various valuesof themagnetic parameter M and in some fixed values of the other dimensionless parameter $S, K1$.

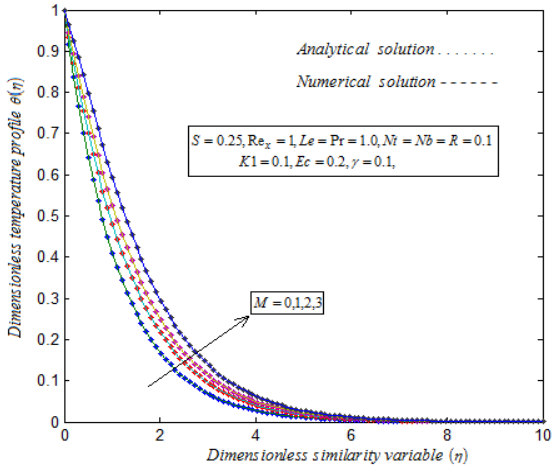

Fig. 3(a): Dimensionless temperature profile $\theta(\eta)$ verses the dimensionless similarity variable (η) .The curves are plotted using the eqn. (23) for various values of the magnetic parameter M and in some fixed values of the other dimensionless parameters $S, K1, \mathrm{Re}_x, Nt, Nb, R, Ec, \mathrm{Pr}, \gamma, Le$.

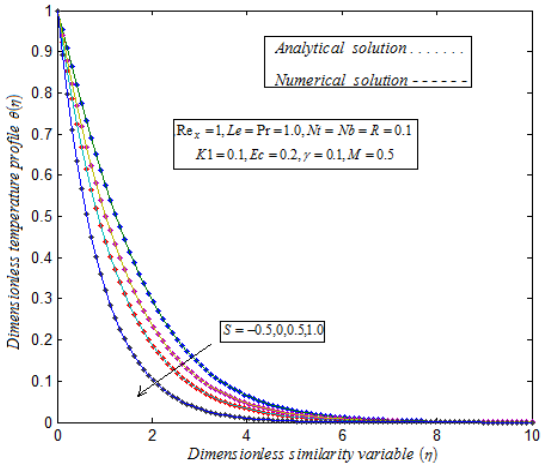

Fig. 3(b): Dimensionless temperature profile $\theta(\eta)$ verses the dimensionless similarity variable (η) .The curves are plotted using the eqn.(23) for various valuesof thesuction parameter S and in some fixed values of the other dimensionless parameter $M, K1, \mathrm{Re}_x, Nt, Nb, R, Ec, \mathrm{Pr}, \gamma, Le$.

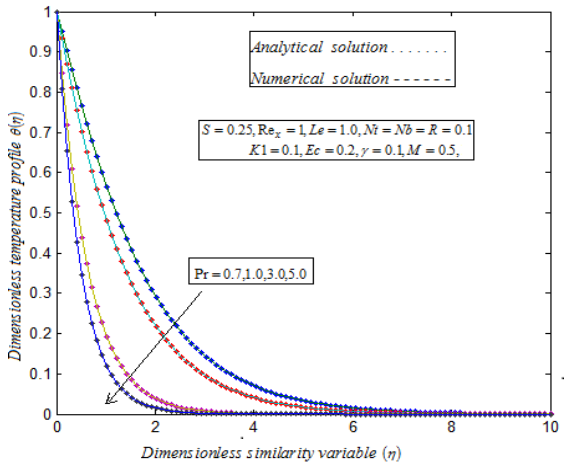

Fig. 3(c): Dimensionless temperature profile $\theta(\eta)$ verses the dimensionless similarity variable (η) .The curves are plotted using the eqn.(23) for various valuesof thePrandtl number $\Pr$ and in some fixed values of the other dimensionless parameter $M, K1, \mathrm{Re}_x, Nt, Nb, R, Ec, \gamma, Le$.

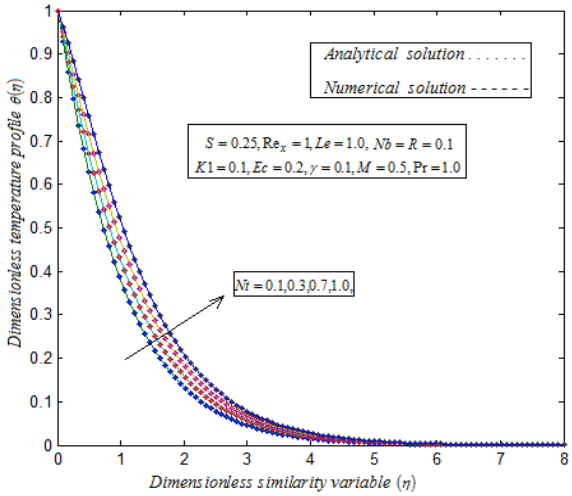

Fig. 3(d): Dimensionless temperature profile $\theta(\eta)$ verses the dimensionless similarity variable (η) .The curves are plotted using the eqn. (23) for various valuesof thethermophoresis parameter Nt and in some fixed values of the other dimensionless parameter $M, K1, \mathrm{Re}_x, Nb, R, Ec, \gamma, Le$.

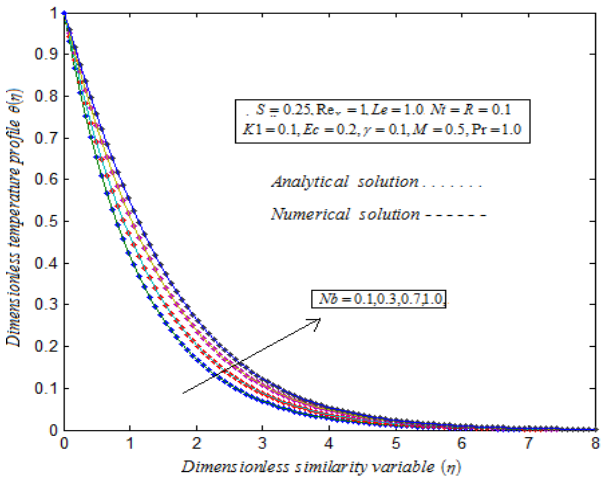

Fig. 3(e): Dimensionless temperature profile $\theta(\eta)$ verses the dimensionless similarity variable (η).The curves are plotted using the eqn. (23) for various valuesof the Brownian motion parameter Nb and insome fixed values of the other dimensionless parameter $M, K1, \mathrm{Re}_x, Nt, R, Ec, \gamma, Le$.

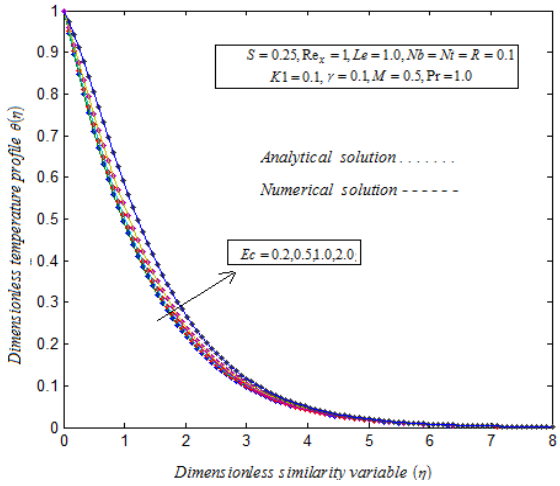

Fig. 3(f): Dimensionless temperature profile $\theta(\eta)$ verses the dimensionless similarity variable (η) .The curves are plotted using the eqn. (23) for various valuesof theEckert number Ec and in some fixed values of the other dimensionless parameter $M, K1, \mathrm{Re}_x, S, Nt, R, Nb, \gamma, Le$.

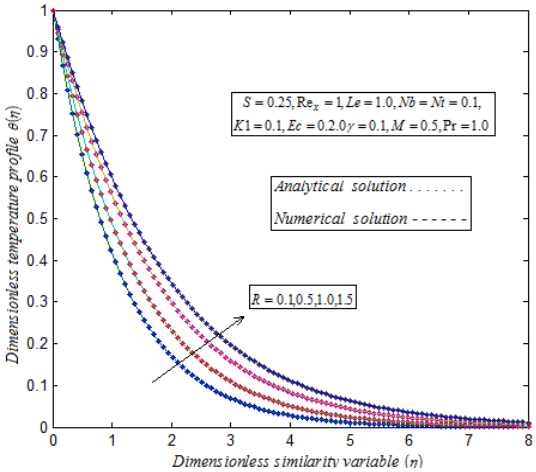

Fig. 3(g): Dimensionless temperature profile $\theta(\eta)$ verses the dimensionless similarity variable (η).The curves are plotted using the eqn.(23) for various valuesof theradiation parameter R and in some fixed values of the other dimensionless parameter $M, K1, \mathrm{Re}_x, Nt, Nb, S, Ec, \gamma, Le$.

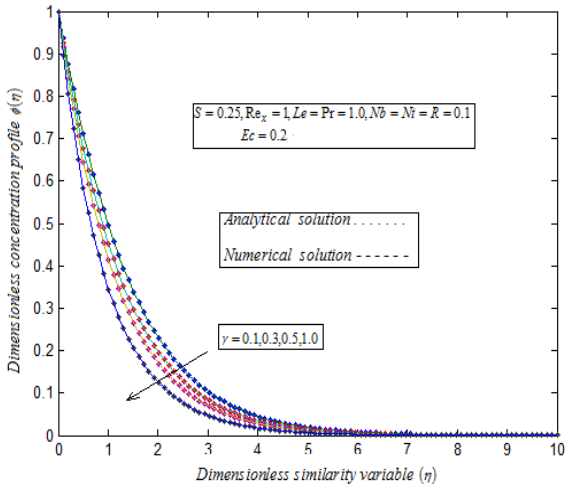

Fig. 4(a): Dimensionless concentration profile $\phi(\eta)$ verses the dimensionless similarity variable (η) .The curves are plotted using the eqn. (24) for various values of the chemical reaction parameter γ and in some fixed values of the other dimensionless parameter $M, K1, \mathrm{Re}_x, Nt, R, Ec, S, Le.$

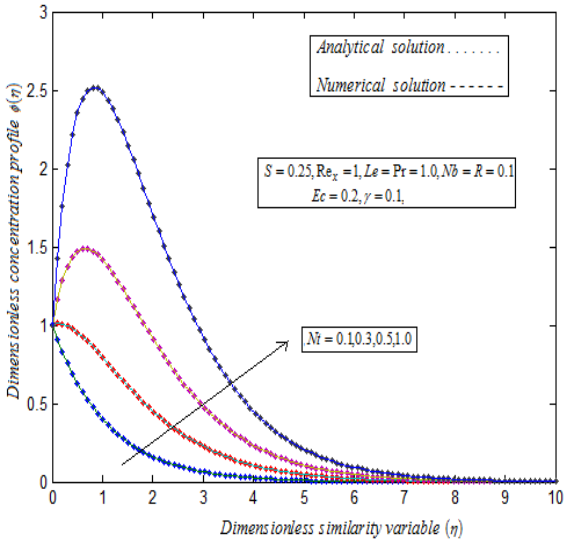

Fig. 4(b): Dimensionless concentration profile $\phi(\eta)$ verses the dimensionless similarity variable (η) .The curves are plotted using the eqn. (24) for various values of the thermophoresis parameter Nt and in some fixed values of the other dimensionless parameter $M, K1, \mathrm{Re}_x, Nb, \gamma, R, Ec, S, Le.$

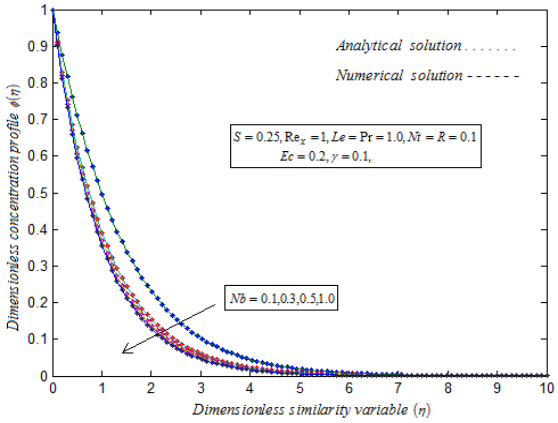

Fig. 4(c): Dimensionless concentration profile $\phi(\eta)$ verses the dimensionless similarity variable (η) .The curves are plotted using the eqn. (24) for various values of the Brownian motion parameter Nb and in some fixed values of the other dimensionless parameter $M, K1, \mathrm{Re}_x, Nt, R, Ec, S, Le, \gamma$.

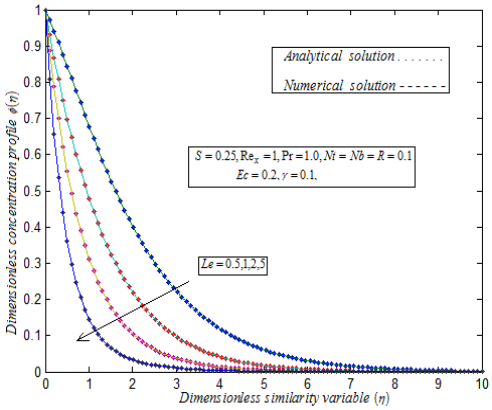

Fig. 4(d): Dimensionless concentration profile $\phi(\eta)$ verses the dimensionless similarity variable (η) .The curves are plotted using the eqn. (24) for various values of the lewis number Le and in some fixed values of the other dimensionless parameter $M, K1, \mathrm{Re}_x, Nt, R, Ec, S, Le, \gamma$.

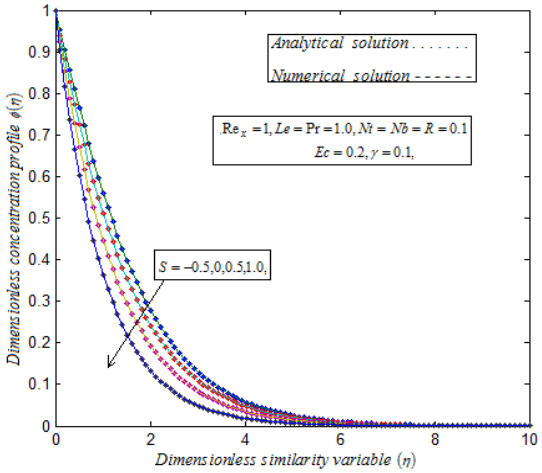

Fig. 4(e): Dimensionless concentration profile $\phi(\eta)$ verses the dimensionless similarity variable (η) .The curves are plotted using the eqn. (24) for various values of the suction parameter S and in some fixed values of the other dimensionless parameter $M, K1, \mathrm{Re}_x, Nt, R, Ec, Nb, Le, \gamma$.

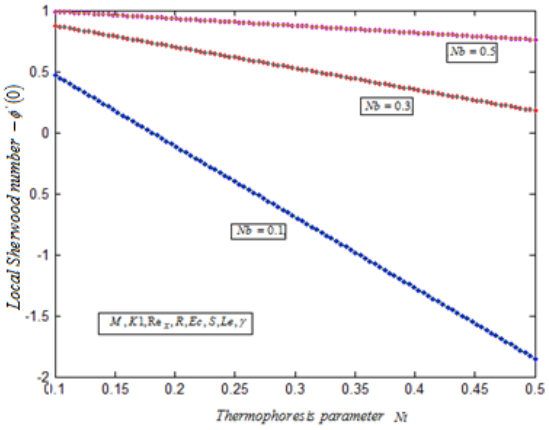

Fig. 4(f): Localsherwood number $-\phi'(0)$ verses thermophoresis parameter Nt .The curves are plotted using the eqn. (27) for various values of the Brownian motion parameter Nb and in some fixed values of the other dimensionless parameter $M, K1, \mathrm{Re}_x, R, Ec, Le, \gamma$.

Table:1 Analytical and numerical values of local skin friction

local skin friction $-f''(0)$				
$Ec, \gamma, \Pr,$ Le, Nt, R M, S, Nb	$K1$	0.2	0.5	0.7
	Numericalsolution	1.6579	1.7538	1.8145
	Analytical solution	1.772	1.861	1.918
	Error %	-0.06	-0.057	-0.053
$Ec, \gamma, \Pr,$ Le, Nt, R M, Nb	S	-0.2	0.2	0.4
	Numerical solution	1.4090	1.5988	1.7042
	Analytical solution	1.515	1.715	1.824
	Error %	-0.069	-0.131	-0.065
$Ec, \gamma, \Pr,$ Le, Nt, R S, Nb	M	0.1	0.5	1
	Numerical solution	1.4822	1.6245	1.7844
	Analytical solution	1.613	1.742	1.890
	Error %	-0.081	-0.067	-0.558

Table.2

local nusselt number $-\theta'(0)$				
$Ec, \gamma, \Pr,$ $Le, Nt, Nb,$ $M, S, K1$	R	0.1	0.2	0.5
	Numerical solution	0.8481	0.7837	0.6419
	Analytical solution	0.8481	0.7831	0.6416
	Error %	0	0.00076	0.0004
$R, \gamma, \Pr,$ $Le, Nt, Nb,$ $M, S, K1$	Ec	0.1	0.3	0.5
	Numerical solution	0.8721	0.8241	0.7762
	Analytical solution	0.8722	0.8223	0.7756
	Error %	-0.0001	0.0021	0.0007
$Ec, R, \Pr,$ $Le, Nt, Nb,$ $M, S, K1$	γ	0.3	0.5	1.0
	Numerical solution	0.8442	0.8416	0.8371
	Analytical solution	0.8441	0.8420	0.8382

	Error %	0.0001	-0.0004	-0.0013
$Ec, \gamma, R,$ $Le, Nt, Nb,$ $M, S, K1$	Pr	1	2	5
	Numerical solution	0.8481	1.3503	2.3631
	Analytical solution	0.8481	1.351	2.310
	Error %	0	-0.0007	0.0229
$Ec, \gamma, \Pr,$ $R, Nt, Nb,$ $M, S, K1$	Le	1	3	5
	Numerical solution	0.8481	0.8291	0.8219
	Analytical solution	0.8481	0.8282	0.8222
	Error %	0	0.0010	-0.0003
$Ec, \gamma, \Pr,$ $R, Nb,$ $M, S, K1$	Nt	0.1	0.3	0.5
	Numerical solution	0.8481	0.8146	0.7834
	Analytical solution	0.8481	0.8125	0.7842
	Error %	0	0.0031	-0.0010
$Ec, \gamma, \Pr,$ $Le, R, Nt,$ $M, S, K1$	Nb	0.1	0.3	0.5
	Numerical solution	0.8481	0.7852	0.7267
	Analytical solution	0.8481	0.7847	0.7248
	Error %	0	0.0006	0.002
$Ec, \gamma, \Pr,$ Le, Nt, R M, S, Nb	$K1$	0.2	0.5	0.7
	Numerical solution	0.8420	0.8247	0.8140
	Analytical solution	0.8422	0.8220	0.8120
	Error %	-0.0002	0.0032	0.0024
$Ec, \gamma, \Pr,$ Le, Nt, R M, Nb	S	-0.2	0.2	0.4
	Numerical solution	0.6418	0.8229	0.9269
	Analytical solution	0.6415	0.8216	0.9265
	Error %	0.0004	0.0015	0.0004

Table.3

local sherwood number $-\phi'(0)$				
$Ec, \gamma, \Pr,$ $Le, Nt, Nb,$ $M, S, K1$	R	0.1	0.2	0.5
	Numerical solution	0.5484	0.5986	0.7070
	Analytical solution	0.5485	0.5989	0.7078
	Error %	0	-0.0005	-0.0011
$Ec, R, \Pr,$ $Le, Nt, Nb,$ $M, S, K1$	γ	0.3	0.5	1.0
	Numerical solution	0.7319	0.8463	1.1564
	Analytical solution	0.7305	0.8422	1.177
	Error %	0.0019	0.0048	-0.0175
$Ec, \gamma, R,$ $Le, Nt, Nb,$ $M, S, K1$	Pr	1	2	5
	Numerical solution	0.5484	0.1390	-0.7556
	Analytical solution	0.5485	0.1389	-0.7446
	Error %	0.0001	0.0007	0.0147

$Ec, \gamma, \Pr,$ $R, Nt, Nb,$ $M, S, K1$	Le	1	3	5
	Numerical solution	0.5484	1.9390	2.971
	Analytical solution	0.5485	1.9392	2.971
	Error %	-0.0001	-0.0001	0
$Ec, \gamma, \Pr,$ $R, Nb,$ $M, S, K1$	Nt	0.1	0.3	0.5
	Numerical solution	0.5484	-0.4984	-1.4496
	Analytical solution	0.5485	-0.4988	-1.446
	Error %	-0.0001	-0.0008	-0.002
$Ec, \gamma, \Pr,$ $Le, R, Nt,$ $M, S, K1$	Nb	0.1	0.3	0.5
	Numerical solution	0.5484	0.9416	1.0194
	Analytical solution	0.5485	0.9418	1.011
	Error %	-0.0001	-0.0002	0.0079

5.Conclusion

A mathematical analysis of the effect of chemical reaction, thermal radiation and viscous dissipation on steady MHD boundary layer flow of nanofluid over an exponentially permeable stretching sheet has been investigated.The approximate analytical expressions of the dimensionless velocity, dimensionless temperature, dimensionless concentration are derived analytically and graphicallywith help of New Homotopy analysis method (NHAM).We can also derived the analytical expressions of local skin friction, local nusselt number and local sherwood number. The skin-friction coefficient, the rate of heat transfer and the rate of mass transferare presented in the tabular form. A good agreement between the analytical and numerical results are observed. This New Homotopy analysis method can be easily extended to solve other non -linear boundary value problems in physical and chemical sciences.

References

[1] Y. Dharmendra Reddy, V. SrinivasaRaoandL.AnandBabu., MHD boundary layer flow of nanofluid and heat transfer over a porous exponentially stretching sheet in presence of thermal radiation and chemical reaction with suction,International Journal of Mathematics Trends and Technology,47,87-100, (2017).

[2] L. J. Crane., Flow past a stretching plate, Journal of Applied Mathematics and Physics, 21, 4, 645 647, (1970).

[3] K. Jafar, R. Nazar, A. Ishak, I. Pop., MHD flow and heat transfer over stretching/shrinking sheets with external magnetic field, viscous dissipation and Joule Effects, CanadianJournal of ChemicalEngineering.5, 1336-1346, (2012).

[4] K.V. Prasad, D. Pal, V. Umesh, N.S. PrasannaRao., The effect of variable viscosity on MHD viscoelastic fluid flow and heat transfer over a stretching sheet, Communication of Nonlinear Science and Numerical Simulation.15, 331-334, (2010).

[5] G. Singh and P.R. Sharma., Effects of Variable Thermal Conductivity and Heat Source / Sink on MHD Flow Near a Stagnation Point on a Linearly Stretching Sheet, Journal of Applied FluidMechanics, 2, 13-21, (2009).

[6] S. U. S. Choi., Enhancing thermal conductivity of fluids with nanoparticles in Development and Applications of Non- Newtonian Flows, AMSE International Mechanical Engineering Congress and Exposition, 12-17, (1995).

[7] W.A. Khan, I. Pop., Boundary layer flow of a nanofluid past a stretching sheet, InternationalJournal of Heatand Mass Transfer.53, 2477–2483, (2010).

[8] S.Naramgari and C. Sulochana.,MHD flow over a permeable stretching/shrinking sheet of a nanofluid with suction/injection, Alexandria Engineering Journal,55,819–827,(2016).
[9] S.Nadeem and C. Lee., Boundary layer flow of nanofluid over an exponentially stretching surface, Nanoscale Research Letters, 7,94-102, (2012).
[10] R. NorfifahBachok, A. L. Pop., Boundary layer stagnation-point flow and heat transfer over an exponentially stretching/shrinking sheet in a nanofluid, International Journalof Heat and Mass Transfer 55, 8122–8128, (2012).
[11] W. Ibrahim, Bandari Shankar., MHD boundary layer flow and heat transfer of a nanofluid past a permeable stretching sheet with velocity thermal and solute slip boundary Conditions, Computers & Fluids 75, 1–10, (2013).
[12] M.M. Rashidi, N. Freidoonimehr and A. Hosseini O. Anwar Bég., T.-K. Hung, Homotopy simulation of nanofluid dynamics from a non-linearly stretching isothermal permeable sheet with transpiration, Mechanics, 49:469–482, (2014).
[13] M.Sheikholeslami, S.Abelman and D.DomiriGanji., Numerical simulation of MHD nanofluid flow and heat transfer considering viscous dissipation, International Journal of Heat and Mass Transfer 79, 212–222, (2014).
[14] Sin Wei Wong, M. A. Omar Awang, Anuar Ishak and Ioan Pop., Boundary Layer Flow and Heat Transfer over an Exponentially Stretching/Shrinking Permeable Sheet with Viscous Dissipation, Journal of Aerospace Engineering, 27, (2014).
[15] Y.YirgSa and D. Tesfaye., Heat and mass transfer in MHD flow of nanofluids through a porous media due to a permeable stretching sheet with viscous dissipation and chemical reaction effects, International Journal of Mechanical, Aerospace, Industrial, Mechatronic and Manufacturing Engineering, 9, 5, (2015).
[16] R. Mutuku-Njane and O.D. Makinde., Heat transfer analysis of MHD nanofluid flow over apermeable plate, Journal of ComputationalTheoretical. Nanoscience, 11,.3, (2014).
[17] F. M. Hady, F.S. Ibrahim,S.M Abdel-Gained and Mohamed R Eid, Radiation effect on viscous flow of a nanofluid and heat transfer over a nonlinearly stretching sheet,Nanoscale ResearchLetters abbreviation., 7(1): 229, (2012).
[18] L. Zhenga, J. Zhang., Flow and radiation heat transfer of a nanofluid over a stretching sheet with velocity slip and temperature jump in porous medium, Journal of the Franklin Institute 350, 990–1007, (2013).
[19] A. S. Dogonchi and D. DomiriGanji., Thermal radiation effect on the Nano-fluid buoyancy flow and heat transfer over a stretching sheet considering Brownian motion, Journal of Molecular Liquids, 223, 521-527, (2016).
[20] E. H. Aly., Radiation and MHD Boundary Layer Stagnation-Point of Nanofluid Flow towardsa Stretching Sheet Embedded in a Porous Medium: Analysis of Suction/Injection andHeat Generation/Absorption with Effect of the Slip Model, Mathematical Problems in Engineering, Article ID 563547, 20 pages, (2015).
[21] M. Imtiaz, T. Hayat and A. Alsaedi., Flow of magneto nanofluid by a radiative exponentiallystretching surface with dissipation effect, Advanced Powder Technology, 27, 2214-2222, (2016).
[22] N. G. Rudraswamy, B. J. Gireesha., Influence of Chemical Reaction and Thermal Radiation on MHD Boundary Layer Flow and Heat Transfer of a Nanofluid over an exponentiallyStretching Sheet, Journal of Applied Mathematics and Physics, 2, 24-32, (2014).
[23] M. R. Eid., Chemical reaction effect on MHD boundary-layer flow of two-phase nanofluid model over an exponentially stretching sheet with a heat generation, Journal of Molecular Liquids, Volume 220, Pages 718–72, (2016).
[24] M. Das,B.K. Mahatha and R. Nandkeolyar., Mixed Convection and Nonlinear Radiation in theStagnation Point Nanofluid flow towards a Stretching Sheet with Homogenous-Heterogeneous Reactions effects, Procedia Engineering, Volume 127, 1018-1025, (2015).
[25] P.Sreedevi, P. Sudarsana Reddy andA.J.Chamkha., Heat and mass transfer analysis ofnanofluid over linear and non-linear stretching surfaces with thermal radiation and chemicalreaction, Powder Technology, 315, 194–204, (2017).
[26] S. J. Liao., beyond perturbation introduction to the Homotopy analysis method, 1st edn, Chapman and Hall, CRC press, Boca Raton, 67,336, (2003).

[27] S. J. Liao., On the Homotopy analysis method for nonlinear problems, Application of Mathematical Computations, 147,499-513 (2004).
[28] S. J. Liao., An optimal Homotopy-analysis approach for strongly nonlinear differential equations, Nonlinear Science and Numerical Simulation,15,2003-2016, (2010).
[29] S. J. Liao., The Homotopy analysis method in non -linear differential equations, Springer and Higher education press, 67, (2012).
[30] S. J. Liao., An explicit totally analytic approximation of Basis viscous flow problems, International journal of Nonlinear Mechanics,34, 759–78, (1999).
[31] S. J. Liao., on the analytic solution of magnetohydrodynamicflows non-Newtonian fluids over a stretching sheet, Journal of Fluid Mechanics, 488,189–212, (2003).
[32] S. J. Liao., A new branch of boundary layer flows over a permeable stretching plate, International Journal of Non-Linear Mechanics. 4219–30, (2007):
[33] S. J. Liao., The proposed Homotopy analysis technique for the solution of nonlinearProblems, Ph.D. Thesis, Shanghai Jiao Tong University, (1992).
[34] S. J. Liao., An approximate solution technique which does not depend upon small Parameters: a special example, International Journal of Non-Linear Mechanics.30 371 380, (1995).

Appendix A

Approximate analytical expression of the non-linear differential eqns. (14) - (16)using ModifiedHomotopy analysis method [25-33]

In this section we derive the analytical expressions of $f(\eta), \theta(\eta)$ and $\phi(\eta)$ using theModified Homotopyanalysis method (MHAM) .

We construct the Homotopy for the eqns.(14)-(16) are as follows:

$$(1-p)\left(\frac{d^3f}{d\eta^3}+S\frac{d^2f}{d\eta^2}-(2+M+K1)\frac{df}{d\eta}\right)=hp\left(\frac{d^3f}{d\eta^3}+S\frac{d^2f}{d\eta^2}-(2+M+K1)\frac{df}{d\eta}\right) \text{(B.1)}$$

$$(1-p)\left(\frac{d^2\theta}{d\eta^2}-\frac{\Pr}{\left(1+\frac{4}{3}R\right)}\theta\right)=h\,p\left(\left(\frac{d^2\theta}{d\eta^2}+\frac{\Pr}{\left(1+\frac{4}{3}R\right)}\left(\begin{array}{l}S\frac{d\theta}{d\eta}-\theta+Ec\left(\frac{d^2f}{d\eta^2}\right)^2\\ +Nb\frac{d\theta}{d\eta}\frac{d\phi}{d\eta}+Nt\left(\frac{d\theta}{d\eta}\right)^2\end{array}\right)\right) \quad \text{(B.2)}$$

$$(1-p)\left(\frac{d^2\phi}{d\eta^2}-(Le+Le\gamma\,\mathrm{Re}_x)\phi\right)=h\,p\left(\left(\begin{array}{l}\frac{d^2\phi}{d\eta^2}+Le\left(S\frac{d\phi}{d\eta}-\phi+\frac{Nt}{Nb}\left(\frac{d^2\theta}{d\eta^2}\right)\right)\\ -Le\gamma\,\mathrm{Re}_x\phi\end{array}\right)\right) \text{(B.3)}$$

The initial approximation for eqns. (14) -(16) is as follows:

$f_0(0)=S,\ f_0(1)=1,\ f_0(\infty)=0$ (B.4)

$\theta_0(0)=1, \theta_0(\infty)=0$ (B.5)

$\theta_0(0)=1, \theta_0(\infty)=0$ (B.6)

$\theta_i(0)=0, \theta_i(\infty)=0 \quad i=1,2,3...n$ (B.7)

$\phi_0(0)=1, \phi_0(\infty)=0$ (B.8)

$\phi_i(0)=0, \phi_i(\infty)=0 \quad i=1,2,3...n$ (B.9)

The approximate solutions for (B.1)– (B.3) are given by

$f = f_0 + pf_1 + p^2 f_2 + ...$ (B.10)

$\theta = \theta_0 + p\theta_1 + p^2\theta_2 + ...$ (B.11)

$\phi = \phi_0 + p\phi_1 + p^2\phi_2 + ...$ (B.12)

By substituting the eqns. (B.10)-(B.12) into the eqns.(B.1)-(B.3) we get

$$(1-p)\left(\begin{array}{l}\frac{d^3\left(f_0+pf_1+p^2f_2+...\right)}{d\eta^3}+S\frac{d^2\left(f_0+pf_1+p^2f_2+...\right)}{d\eta^2}\\-(2+M+K1)\frac{d\left(f_0+pf_1+p^2f_2+...\right)}{d\eta}\end{array}\right) \quad \text{(B.13)}$$

$$=hp\left(\begin{array}{l}\frac{d^3\left(f_0+pf_1+p^2f_2+...\right)}{d\eta^3}+S\frac{d^2\left(f_0+pf_1+p^2f_2+...\right)}{d\eta^2}\\-(2+M+K1)\frac{d\left(f_0+pf_1+p^2f_2+...\right)}{d\eta}\end{array}\right)$$

$$(1-p)\left(\frac{d^2\left(\theta_0+p\theta_1+p^2\theta_2+..\right)}{d\eta^2}-\frac{\Pr\left(\theta_0+p\theta_1+p^2\theta_2+..\right)}{\left(1+\frac{4}{3}R\right)}\right)$$

$$=h\,p\left(\left(\begin{array}{l}\frac{d^2\left(\theta_0+p\theta_1+p^2\theta_2+..\right)}{d\eta^2}\\+\frac{\Pr}{\left(1+\frac{4}{3}R\right)}\left(\begin{array}{l}S\frac{d\left(\theta_0+p\theta_1+p^2\theta_2+..\right)}{d\eta}+Ec\left(\frac{d^2\left(f_0+pf_1+p^2f_2+..\right)}{d\eta^2}\right)^2\\+Nb\left(\frac{d\left(\theta_0+p\theta_1+p^2\theta_2+..\right)}{d\eta}\right)\left(\frac{d\left(\phi_0+p\phi_1+p^2\phi_2+..\right)}{d\eta}\right)\\+Nt\left(\frac{d\left(\theta_0+p\theta_1+p^2\theta_2+..\right)}{d\eta}\right)^2\end{array}\right)\end{array}\right)\right) \quad \text{(B.14)}$$

$$(1-p)\left(\frac{d^2\left(\phi_0+p\phi_1+p^2\phi_2+..\right)}{d\eta^2}-(Le+Le\gamma\,\mathrm{Re}_x)\left(\phi_0+p\phi_1+p^2\phi_2+..\right)\right)$$

$$=h\,p\left(\left(\begin{array}{l}\frac{d^2\phi_0}{d\eta^2}+Le\left(\begin{array}{l}S\frac{d\phi_0}{d\eta}-\left(\phi_0+p\phi_1+p^2\phi_2+..\right)\\+\frac{Nt}{Nb}\left(\frac{d^2\left(\theta_0+p\theta_1+p^2\theta_2+..\right)}{d\eta^2}\right)\\(-Le\gamma\,\mathrm{Re}_x)\left(\phi_0+p\phi_1+p^2\phi_2+..\right)\end{array}\right)\end{array}\right)\right) \quad \text{(B.15)}$$

Now equating the coefficients of p^0 and p^1 we get the following eqns.

$$p^0=\frac{d^3f_0}{d\eta^3}+S\frac{d^2f_0}{d\eta^2}-(2+M+K1)\frac{df_0}{d\eta}=0 \quad \text{(B.16)}$$

$$p^0=\frac{d^2\theta_0}{d\eta^2}-\frac{\Pr}{\left(1+\frac{4}{3}R\right)}\theta_0=0 \quad \text{(B.17)}$$

$$p^1=\frac{d^2\theta_1}{d\eta^2}-\frac{\Pr}{\left(1+\frac{4}{3}R\right)}\theta_0+\frac{\Pr}{\left(1+\frac{4}{3}R\right)}\left(\begin{array}{l}S\frac{d\theta_0}{d\eta}+Ec\left(\frac{d^2{f_0}^2}{d\eta^2}\right)\\+\left(\frac{d\theta_0}{d\eta}\right)\left(\frac{d\phi_0}{d\eta}\right)+Nt\left(\frac{d\theta_0}{d\eta}\right)^2\end{array}\right)=0 \quad \text{(B.18)}$$

$$p^0=\frac{d^2\phi_0}{d\eta^2}-(Le+Le\,\mathrm{Re}_x\gamma)\phi_0=0 \quad \text{(B.19)}$$

$$p^1 = \frac{d^2\phi_1}{d\eta^2} - \left(Le + Le\,\gamma\,\mathrm{Re}_x\right)\phi_1 + \left(Le\left(S\frac{d\phi_0}{d\eta} + \frac{Nt}{Nb}\left(\frac{d^2\theta_0}{d\eta^2}\right)\right)\right) = 0 \text{ (B.20)}$$

Solving (B.16)- (B.20) by using the boundary condition (B.4) -(B.9) obtain the following results,

$$f_0(\eta) = e_1 + e_2\, e^{G\eta} + e_3\, e^{-G_1\eta} \text{ (B.21)}$$

$$\theta_0(\eta) = r_1\, e^{L\eta} + r_2\ e^{-L\eta} \text{ (B.22)}$$

$$\theta_1(\eta) = -h\left(\left(r_3\, e^{L\eta} + r_4\, e^{-L\eta}\right) + \frac{\Pr}{\left(1+\frac{4}{3}R\right)} \left[\begin{array}{l} s\left(\frac{-L\,e^{-L\eta}}{L^2-L}\right) + \frac{c^2\,Ec\,e^{-2c\eta}}{\left(4c^2-L\right)} \\ + Nb\left(\left(\frac{-L\,e^{-L\eta}}{L^2-L}\right)\left(\frac{-B\,e^{-B\eta}}{B^2-L}\right)\right) \\ Nt\left(\frac{L^2 e^{-2L\eta}}{\left(4L^2-L\right)}\right) \end{array} \right] \right) \text{ (B.23)}$$

$$\phi_0(\eta) = c_1\, e^{B\eta} + c_2\, e^{-B\eta} \text{ (B.24)}$$

$$\phi_1(\eta) = -h\left[c_3\, e^{B\eta} + c_4\, e^{-B\eta} - \frac{Le\,S\,B\,e^{-B\eta}}{B^2-B} - \frac{Nt}{Nb}\frac{L^2 e^{-L\eta}}{L^2-B} \right] \text{ (B.25)}$$

According to Modified Homotopy analysis method, we have

$$f = \lim_{p\to 1} f(\eta) = f_0 \text{ (B.26)}$$

$$\theta = \lim_{p\to 1} \theta(\eta) = \theta_0 + \theta_1 \text{ (B.27)}$$

$$\phi = \lim_{p\to 1} \phi(\eta) = \phi_0 + \phi_1 \text{ (B.28)}$$

After putting the eqn. (B.21) into an eqn. (B.26), the eqns.(B.22) and (B.23) into an eqn.(B.27)andthe eqns.(B.24)and (B.25) into an eqn.(B.28), we obtain the solutions in the text as given in the eqns. (21), (23) and (24) respectively.

Appendix B
Nomenclature

Symbols	Meaning
Sh_x	Sherwood number
Nu_x	Nusselt number
$B(x)$	Magnetic field strength
C	Nano particle concentration
Cf_x	Skin-friction coefficient
C_w	Nano particles concentration at the stretching surface
C_∞	Nano particle concentration far from the sheet
C_P	Specific heat capacity at constant pressure
U_w	Velocity of the wall along the x-axis
u, v	Velocity components in the x- and y axis, respectively
D_∞	Thermophoresis diffusion coefficient

k^*	Roseland mean absorption coefficient
k	Thermal conductivity
Le	Lewis number
M	Magnetic parameter
S	Suction/ Injection parameter
D_T	Brownian diffusion coefficient
Nt	Thermophoresis parameter
Nb	Brownian motion parameter
Re_x	local Reynolds number
γ	chemical reaction parameter
R	radiation parameter
$K1$	permeability parameter
Ec	Eckert number
Pr	Prandtl Number
M	Magnetic parameter